

# Magnetic fields of spherical, cylindrical, and ellipsoidal electric charge superficial distributions at rotation

M.A. Avila\*

*Facultad de Ciencias, Universiada Autónoma del Estado de Morelos,  
Apartado Postal 62210, Cuernavaca, Morelos, Mexico.*

\* *e-mail: avila@servm.fc.uaem.mx*

Recibido el 12 de marzo de 2002; aceptado el 6 de septiembre de 2002

The vector potentials  $\mathbf{A}(\mathbf{r})$  produced by spherical, cylindrical, and ellipsoidal uniform superficial distributions of electrical charge rotating at a constant angular velocity  $\omega$ , are found. This is done by modeling such a distributions as if they were simple bobbins made of  $N$  loops of a very thin coil carrying a current  $I$  and calculating simply the dipolar potential  $\mathbf{A}_{\text{dip}}(\mathbf{r})$  produced by them. Due that in the case of the spherical geometry the potential  $\mathbf{A}(\mathbf{r})$  has already been calculated its value is used as a consistence test of the present approach, for the two other geometries the analytical calculation of the potentials is not so trivial by this reason the equalness between  $\mathbf{A}_{\text{dip}}(\mathbf{r})$  and  $\mathbf{A}(\mathbf{r})$  is proved trough a numerical evaluation of the complex integrals appearing in the Biot-Savart expression for  $\mathbf{A}(\mathbf{r})$ . The respective magnetic fields generated by these three rotating distributions have an identical structure: they are constant inside the surfaces while outside them they are dipolar-like (nearby to radiation zone). An application of the above results to quark confinement inside hadrons is proposed.

*Keywords:* Rotating charge distribution; magnetic vector potential; bobbins; magnetic dipole expansion; quark confinement; magnetic field.

Se hallan los potenciales vectoriales  $\mathbf{A}(\mathbf{r})$  producidos por distribuciones superficiales de carga eléctrica esferoidales, cilíndricas y elipsoidales rotando en una velocidad angular constante  $\omega$ . Esto es hecho modelando a estas distribuciones como si fueran bobinas de  $N$  vueltas de alambre delgado portando una corriente  $I$  y calculando simplemente los potenciales dipolares  $\mathbf{A}_{\text{dip}}(\mathbf{r})$  producidos por ellas. Debido a que en el caso de la geometría esférica el potencial  $\mathbf{A}(\mathbf{r})$  ya ha sido calculado, su valor es usado como prueba de la consistencia del presente enfoque, para las otras dos geometrías el calculo analítico de los potenciales no es trivial lo cual nos obliga a probar la igualdad entre  $\mathbf{A}_{\text{dip}}(\mathbf{r})$  y  $\mathbf{A}(\mathbf{r})$  a través de una evaluación numérica de las complejas integrales que aparecen en la expresión Biot-Savart para  $\mathbf{A}(\mathbf{r})$ . Los respectivos campos magnéticos generados por estas tres distribuciones rotando tienen la misma estructura: son constantes adentro de ellas mientras que afuera son de tipo dipolar cercana a la zona de radiación. Se propone una aplicación de los anteriores resultados al confinamiento de quarks dentro de hadrones.

*Descriptores:* Distribución rotante de carga; potencial vectorial magnético; bobinas; expansión dipolar; magnética; confinamiento de quark; campo magnético.

PACS: 41.20; 07.55.D

## 1. Introduction

It is well known about the difficulties concerning to the calculation of the exact value of the magnetic vector potential  $\mathbf{A}(\mathbf{r})$  associated to an arbitrary superficial distribution of electric charge  $\sigma$  which is rotating at a constant angular velocity  $\omega$ . In fact, this happens even for uniform and quite symmetrical superficial distributions whereas the only well known existing analytic solution for this kind of devices is that of the spherical distribution [1] and the most it has been done for other different geometries is to find approximate solutions [For points very far away of the sources it is possible to know the values of the potentials  $\mathbf{A}(\mathbf{r})$  of several symmetrical distributions (*e.g.*, cylindrical, ellipsoidal, and conical) of electric charge at uniform rotation [2]]. The main problem for performing these calculations lies in the cumbersome integrals appearing in the Biot-Savart expression for  $\mathbf{A}(\mathbf{r})$ . By focusing on three surfaces (spherical, cylindrical and ellipsoidal) symmetrical enough which are uniformly charged, the purpose of this work is to calculate the vector potentials produced by them when they are rotating at a constant angular velocity. For accomplishing this task we shall go round to the

cumbersome analytical calculation of the integrals appearing in the Biot-Savart expression for  $\mathbf{A}(\mathbf{r})$  and model such a rotating surfaces as if they were bobbins having the same shape that the distributions and made of  $N$  circular loops of a very thin wire carrying a current  $I$ , the vector potentials  $\mathbf{A}(\mathbf{r})$  associated to the rotating surfaces are simply the dipolar potentials  $\mathbf{A}_{\text{dip}}(\mathbf{r})$  produced by these bobbins. The way it is proved the equalness between  $\mathbf{A}(\mathbf{r})$  and  $\mathbf{A}_{\text{dip}}(\mathbf{r})$  is as follows:

- i) In the case of the rotating sphere it is compared the value of  $\mathbf{A}_{\text{dip}}(\mathbf{r})$  as it is predicted by the bobbins model with the already known expression for  $\mathbf{A}(\mathbf{r})$  obtained in Ref. 1 through a formal calculation of the Biot-Savart integral. Since it is found that both expressions coincide, this encourage us to investigate the predictions of the present approach for the cylindrical and ellipsoidal distributions.
- ii) For these two geometries it is evaluated numerically the respective integral appearing in the Biot-Savart expressions for  $\mathbf{A}(\mathbf{r})$  and compared this quantity with  $\mathbf{A}_{\text{dip}}(\mathbf{r})$  finding that the dipolar potentials account very well for the Biot-Savart potentials.

In order to make the numerical integrals independent of some particular value of the dimensions of the distributions it is made a suitable change of coordinates into dimensionless variables. It is necessary to observe that within bobbins image, the uniformity of electric charge on the surfaces ( $\sigma = ct$ ) shall be understood as the condition that the linear density of turns  $\lambda = dN/ds$  of the wire on the bobbins is constant. Likewise, the determination of the values of the several parameters (e.g.,  $\lambda$ ,  $I$ ,  $\sigma$ , etc) involved in the problem shall be done through the assumption that the magnetic dipolar moments must have the same value in both of the images (e.g., bobbins and rotating surfaces). Our conclusions are mainly two, the first one is that through the use of bobbins model it is possible to calculate the previously unsolved  $\mathbf{B} = \nabla \times \mathbf{A}$  fields in a fashion which has the advantage of being mathematically simpler than the method of calculating analytically the non trivial integrals appearing in the Biot-Savart equation, and the other is that the three fields calculated have in common a dipolar-like structure outside the distributions while inside them they are constant.

The way we shall proceed in this work is as follows, in Sec. 1 we give a survey of the known results on circular loops

carrying a current  $I$  then in Sec. 2 it is calculated the dipolar potentials and verify numerically the validity of our approximation. Finally in Sec. 3 it is given a brief discussion of our findings.

### 2. Circular loops

Let us consider a circular bobbin consisting of  $N$  circular loops of radius  $a$  carrying a current

$$\mathbf{J}(\mathbf{r}) = NI \delta(z - H) \delta(\rho - a) \hat{\varphi}$$

with center at the origin and contained in a plane which is parallel to the  $XY$  plane as it is sketched in Fig 1. The dipolar magnetic moment generated by this current distribution is

$$\mathbf{m} = \frac{1}{2} \int d^3\mathbf{l} \quad \mathbf{l} \times \mathbf{J}(\mathbf{l}) = N\pi a^2 I \hat{\mathbf{k}}, \quad (1)$$

while the respective Biot-Savart potential associated to this current is

$$\mathbf{A}(\mathbf{r}) = \frac{\mu_o}{4\pi} \int \frac{\mathbf{J}(\mathbf{l})}{|\mathbf{r} - \mathbf{l}|} = \frac{\mu_o}{4\pi} NIa \left( \int_{\varphi'=0}^{\varphi'=2\pi} \frac{d\varphi' \cos \varphi'}{\sqrt{\rho^2 + a^2 + 2a\rho \cos(\varphi - \varphi') + (z - z')^2}} \right) \hat{\varphi}. \quad (2)$$

In the context of the present approach the above two equations are very useful so they will be used recurrently in the following.

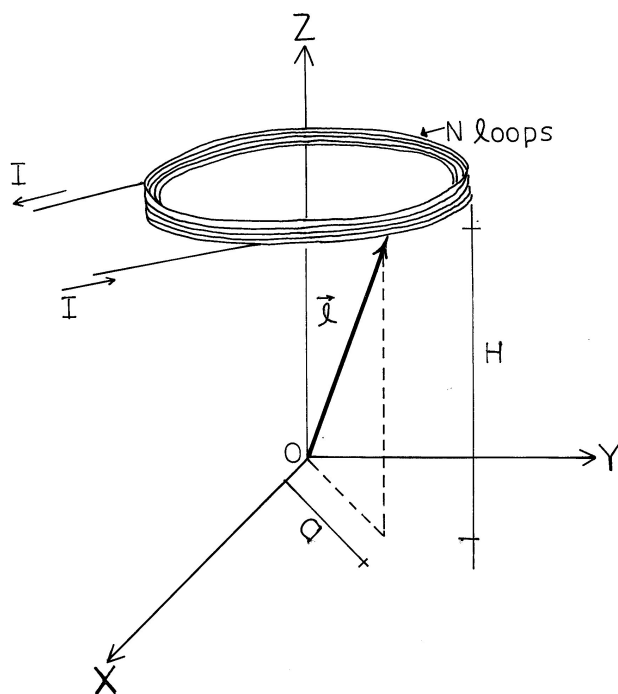


FIGURE 1. Plane circular circuit of  $N$  loops of radius  $a$  parallel to the  $XY$  plane and carrying a current  $I$ .

Let us now proceed to calculate the potentials of interest for us.

### 3. Superficial charge distributions at uniform rotation

An electrical charge  $Q$  uniformly distributed on a surface of particular shape which is rotating with respect to its symmetry axis at a constant angular velocity  $\omega$  will be thought here as a bobbin made of  $N$  loops of coil carrying a constant current  $I$ . The coil will be assumed to be twined around in such a way it preserves the same shape of the rotating distribution. In Figs. 2-4 are shown the three particular superficial (spherical, cylindric and elipsoidal) distributions of electric charge under consideration together with their respective associated bobbins.

#### 3.1. Rotating sphere

According with the stated above, an spherical shell of radius  $R$  having a charge uniformly distributed according to  $\sigma = Q/(4\pi R^2)$  which is spinning round at uniform angular velocity  $\omega$  around  $Z$ - axis will have associated a one layer spherical bobbin of  $N$  turns wrapping up all of the sphere and carrying a constant current  $I = Q\nu = 2\omega\sigma R^2$  [The current density associated to this device is

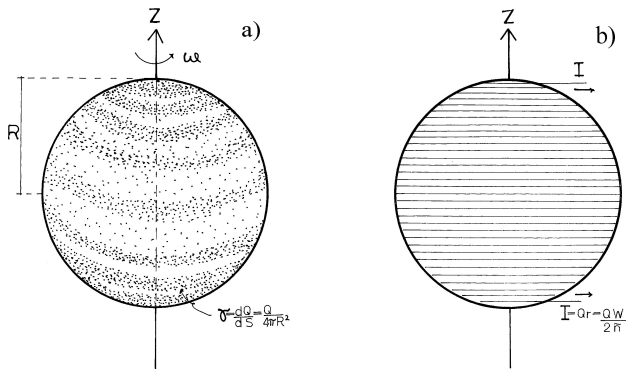


FIGURE 2. (2a) Spherical shell of radius  $R$  rotating uniformly with angular velocity  $\omega$  along  $Z$  axis and containing a charge  $Q$  uniformly distributed on it according to  $\sigma = Q/(4\pi R^2)$ . (2b) Spherical bobbin of radius  $R$  made of  $N$  loops and carrying a current  $I = Q\nu = Q\omega/(2\pi)$ .

$$\mathbf{J}(\mathbf{r}) = \rho\mathbf{v} = \delta(r - R)\sigma\omega\hat{\phi} = \delta(r - R)\frac{I \sin\theta}{2R}\hat{\phi} \quad [1,3].$$

This arrangement is sketched in Fig. 2. The linear density of turns (=number of turns/meter) of the bobbin will be assumed here to be constant at a value

$$\lambda = \frac{dN}{ds} = \frac{1}{R} \frac{dN}{d\theta} = \frac{4}{3} \frac{1}{\pi R}.$$

In order to check the consistency of the present approach, we first calculate the magnetization generated by the  $N$  loops and compare the obtained result with the already known for the rotating sphere found in Ref. 1.

From Eq. (1), the magnetic dipole moment  $d\mathbf{m}$  generated by  $dN = \lambda R d\theta$  turns on the sphere will be

$$d\mathbf{m} = dN\pi\rho^2 I \hat{\mathbf{k}} = \lambda\pi R^3 I \sin^2\theta d\theta \hat{\mathbf{k}}.$$

To be integrated this quantity over all of the distribution, the total dipole moment generated by the  $N$  loops is

$$\mathbf{m} = \frac{1}{2}\lambda\pi^2 R^3 I \hat{\mathbf{k}}.$$

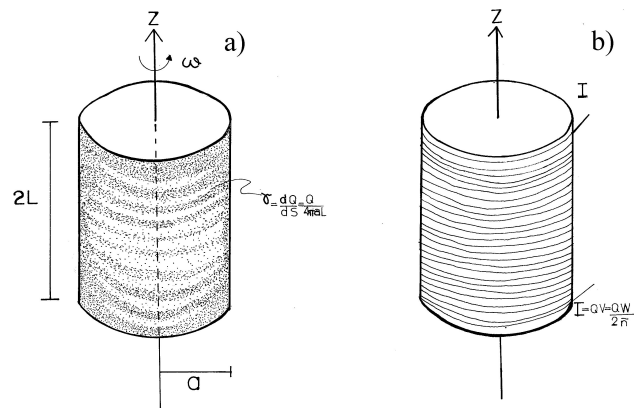


FIGURE 3. (3a) Cylindrical shell of radius  $a$  and height  $2L$  rotating uniformly with angular velocity  $\omega$  along  $Z$  axis and containing a charge  $Q$  uniformly distributed on it according to  $\sigma = Q/(4\pi aL)$ . (3b) Cylindrical bobbin of radius  $a$  and height  $2L$  made of  $N$  loops and carrying a current  $I = Q\nu = Q\omega/(2\pi)$ .

This value for  $\mathbf{m}$  leads to a magnetization

$$\mathbf{M} = \frac{\mathbf{m}}{(4/3)\pi R^3} = \sigma\omega R \hat{\mathbf{k}}. \quad (3)$$

One must observe that the above values for both  $\mathbf{m}$  and  $\mathbf{M}$  coincide with those found in Ref. 1 through a quite lengthy calculation of the integral

$$\mathbf{m} = \frac{1}{2} \int d^3\mathbf{l} \quad \mathbf{l} \times \mathbf{J}(\mathbf{l}).$$

This encouraging result indicates a good signal of consistence of our approach.

In order to proceed further, let us now calculate the respective value of the dipole vector potential  $\mathbf{A}_{\text{dip}}(\mathbf{r})$  produced by  $\mathbf{m}$ .

By using cylindrical coordinates (with the respective replacement  $a = \rho'$ ) in Eq. (2) the potential produced by the  $N$  turns twined around the surface of the sphere will be

$$\mathbf{A}(\mathbf{r}) = \frac{\mu_o}{4\pi} \lambda R^2 I \hat{\phi} \left( \int_{\theta'=0}^{\theta'=\pi} d\theta' \sin\theta' \int_{\varphi'=0}^{\varphi'=2\pi} \frac{d\varphi' \cos\varphi'}{\sqrt{r^2 + R^2 - 2[\rho\rho' \cos(\varphi - \varphi') + zz']}} \right) \hat{\phi}. \quad (4)$$

In order to evaluate adequately the above integral it is necessary to consider two different cases.

### 3.1.1. $\mathbf{A}(\mathbf{r})$ inside the sphere: $r \leq R$

By making an expansion in powers of  $\frac{r}{R}$  in Eq. (4) it is obtained

$$\mathbf{A}(\mathbf{r}) = \frac{\mu_o}{4\pi} \lambda R^2 I \hat{\phi} \int_{\theta'=0}^{\theta'=2\pi} d\theta' \sin\theta' \int_{\alpha=-\varphi}^{\alpha=-\varphi+2\pi} d\alpha \cos\alpha \left\{ 1 - \frac{1}{2} \left[ \left( \frac{r}{R} \right)^2 - 2 \left( \frac{\rho}{R} \cos\alpha \sin\theta' + \frac{zz'}{R^2} \right) \right] \right. \\ \left. + \frac{3}{8} \left[ \left( \frac{r}{R} \right)^2 - 2 \left( \frac{\rho}{R} \cos\alpha \sin\theta' + \frac{zz'}{R^2} \right) \right]^2 - \frac{5}{16} \left[ \left( \frac{r}{R} \right)^2 - 2 \left( \frac{\rho}{R} \cos\alpha \sin\theta' + \frac{zz'}{R^2} \right) \right]^3 - \dots \right\}. \quad (5)$$

As it is easily observed in the last equation, the two first integrals vanish while the third one also called dipolar term, does not. In fact this term leads to a dipolar potential  $\mathbf{A}_{\text{dip}}(\mathbf{r}) = (\mu_o\pi/8)\lambda I\rho\hat{\varphi}$ . By using that

$$\lambda = \frac{4}{3} \frac{1}{\pi R} \quad \text{and} \quad I = \frac{Q\omega}{2\pi},$$

the potential inside the spherical bobbin will take the form

$$\mathbf{A}_{\text{dip}}(\mathbf{r}) = \frac{\mu_o R \omega \sigma}{3} r \sin \theta \hat{\varphi} \quad 0 \leq r \leq R. \quad (6)$$

The above dipolar potential is exactly the same to the Biot-Savart potential of the rotating spherical distribution found in Ref. 1. This coincidence indicates that our approach works very well (at least for the internal region of the sphere) and incidentally save us the cumbersome calculation of the Biot-Savart potential generated by the rotating charged sphere.

To make sure that our approach works completely well in the case of the spherical geometry let us study now the other region of interest.

### 3.1.2. $\mathbf{A}(\mathbf{r})$ outside the sphere: $R < r$

After doing an expansion in powers of  $R/r$  in Eq. (4) and keeping only the dipolar term, it is obtained

$$\mathbf{A}_{\text{dip}}(\mathbf{r}) = \frac{\mu_o\pi}{8}\lambda I\left(\frac{R}{r}\right)\rho\hat{\varphi}.$$

Using the prescribed values for  $\lambda$  and  $I$  this potential can be written as

$$\mathbf{A}_{\text{dip}}(\mathbf{r}) = \frac{\mu_o R^4 \omega \sigma}{3} \frac{\sin \theta}{r^2} \hat{\varphi} \quad R < r. \quad (7)$$

This result also coincide exactly with the respective expression for the rotating sphere found in Ref. 1.

### 3.1.3. $\mathbf{A}(\mathbf{r})$ for the rotating sphere.

With Eqs. (6) and (7) the dipolar potential associated to the spherical bobbin can be written in a simplified way as follows

$$\mathbf{A}_{\text{dip}}(\mathbf{r}) = \mathbf{A}(\mathbf{r}) = \frac{\mu_o R \sigma \omega}{3} \begin{cases} \rho \hat{\varphi} & 0 < r \leq R, \\ \frac{R^3}{r^3} \rho \hat{\varphi} & R < r. \end{cases} \quad (8)$$

The coincidence between the values of the dipolar and Biot-Savart potentials, stimulates us to investigate whether if our alternative and simpler approach works well for describing other different geometries at uniform rotation. Let us explore this possibility for both the cylindrical and ellipsoidal distributions.

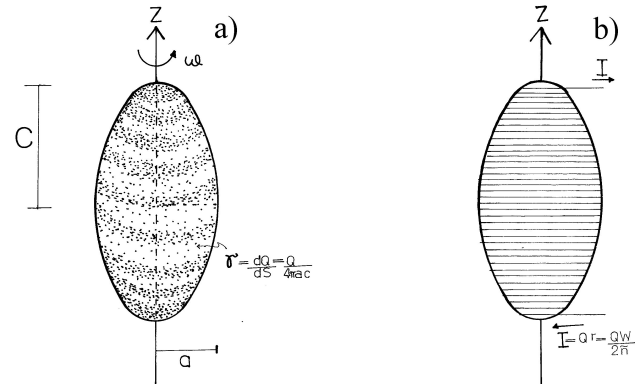


FIGURE 4. (4a) Elipsoidal shell of minor axis  $a$  and major axis  $c$  rotating uniformly with angular velocity  $\omega$  along  $Z$  axis and containing a charge  $Q$  uniformly distributed on it according to  $\sigma = Q/S(e)$  where  $S(e)$  is the ellipsoid area. (4b) Elipsoidal bobbin of radius  $a$  and major axis  $c$  made of  $N$  loops and carrying a current  $I = Q\nu = Q\omega/(2\pi)$ .

## 3.2. Rotating cylinder

Our next goal is now to determine whether if the present method can be applied to the calculation of the vector potential associated to a charge  $Q$  uniformly distributed on the side of a cylinder of height  $2L$  and radius  $a$  which is spinning round at uniform angular velocity  $\omega$  along its symmetry ( $Z$ -)axis. In order to investigate a bit more on this matter let us first calculate the linear density of turns  $\lambda$  associated to a cylindrical bobbin carrying a current  $I$  which will be modeling to the rotating cylinder as it is sketched in Fig 3. The way it is determined  $\lambda$  here is by making equal the value of the magnetic dipole moment of the bobbin (depending on  $\lambda$ ) with the one of the rotating cylindrical surface. This simple procedure is shown below.

Within the image of a cylindrical bobbin of  $N$  turns carrying a current  $I = Q\nu = 2La\omega\sigma$ , the value of the associated magnetic dipole moment will be

$$\begin{aligned} \mathbf{m}_{\text{bobbin}}^{\text{cyl}} &= \int d\mathbf{m} = \int dN\pi a^2 I \hat{\mathbf{k}} \\ &= \lambda \pi a^2 I \int_{z=-L}^{z=+L} dz' \hat{\mathbf{k}} = 2L\pi a^2 I \lambda \hat{\mathbf{k}}. \end{aligned}$$

On the other hand, the magnetic moment generated by the rotating cylinder is the one generated by the current

$$\mathbf{J} = \delta(\rho' - a)\sigma\omega \hat{\mathbf{k}} \times \mathbf{l} = a\omega\delta(\rho' - a)\sigma\hat{\varphi}',$$

that is

$$\mathbf{m}_{\text{rot}}^{\text{cyl}} = \frac{1}{2} \int d^3\mathbf{l} \mathbf{l} \times \mathbf{J} = \pi I a^2 \hat{\mathbf{k}}.$$

Therefore, by making equal the values of  $\mathbf{m}_{\text{rot}}^{\text{cyl}}$  and  $\mathbf{m}_{\text{bobbin}}^{\text{cyl}}$  it is obtained  $\lambda = 1/2L$ . With this value for  $\lambda$ , the corresponding magnetization in both of the images will be

$$\mathbf{M}_{\text{cyl}} = \frac{\mathbf{m}}{2\pi a^2 L} = a\omega\sigma\hat{\mathbf{k}}. \quad (9)$$

Once it is known  $\lambda$ , we are now in position of calculating the value of the dipolar vector potential as it is predicted by the present approach.

According with Eq. (2) the potential associated to a cylindrical bobbin must have the form

$$\begin{aligned} \mathbf{A}(\mathbf{r}) &= \frac{\mu_o}{4\pi} I a \int dN \int \frac{d\varphi' \cos \varphi'}{\sqrt{\mathbf{r}^2 - 2\mathbf{r} \cdot \mathbf{l} + l^2}} \hat{\varphi} \\ &= \frac{\mu_o I \lambda}{4\pi} \int_{z'=-L}^{z'=L} \frac{dz'}{\sqrt{r^2 + l^2}} \int_0^{2\pi} \frac{d\varphi' \cos \varphi'}{\sqrt{1 - \frac{2\mathbf{r} \cdot \mathbf{l}}{r^2 + l^2}}} \hat{\varphi} \end{aligned} \quad (10)$$

where  $l^2 = a^2 + z'^2$ . By making an expansion in powers of  $(2\mathbf{r} \cdot \mathbf{l})/(r^2 + l^2)$  in (9) and keeping only the dipolar term (proportional to the first non vanishing integral) it is obtained the general form for the dipolar potential

$$\mathbf{A}_{\text{dip}}(\mathbf{r}) = \frac{\mu_o}{4\pi} \cdot \frac{\rho}{(r^2 + a^2)\sqrt{r^2 + a^2 + L^2}} \mathbf{m} \times \hat{\rho}, \quad (11)$$

where  $\mathbf{m} = \pi I a^2 \hat{\mathbf{k}}$ .

From the above expression it is obvious that  $\mathbf{A}_{\text{dip}}(\mathbf{r})$  depends on the correlation between the values of  $\rho, z, a$ , and  $L$ . In order to obtain an expression for  $\mathbf{A}_{\text{dip}}(\mathbf{r})$  where it can be seen in a more explicit way its behaviour, we have found convenient to divide the space basically in the four following regions: Inside cylinder ( $0 \leq \rho < a, -L < z < +L$ ), Region I (up and down external parts to cylinder lids:  $0 \leq \rho < a, L < |z|$ ), Region II (external regions to cylinder edges:  $a < \rho, L < |z|$ ), and Region III (external part to cylinder side:  $a < \rho, \leq |z| < L$ ). In the above it is implicitly understood that for each case the azimuthal angle runs over all of its range  $0 \leq \varphi \leq 2\pi$ . In Figure 5 it is sketched this single partition. From this figure one can see that our election lies basically in the dominant spatial quantities characterizing each one of these regions, that is: inside cylinder the dipolar expansion factor must be  $\sqrt{a^2 + L^2}$  because for any field point  $\mathbf{r} = (x, y, z)$  inside it, it holds that  $r = \sqrt{x^2 + y^2 + z^2} \leq \sqrt{a^2 + L^2}$ ; since for any source point  $\mathbf{l}$  on the cylinder it holds that  $l \leq \sqrt{a^2 + L^2}$ , hence in the Region I the corresponding dipolar expansion factor must be  $\sqrt{r^2 + a^2}$  where obviously  $L \leq r$  and; in Region II the expansion parameter is  $r$  because its minimal value is  $\sqrt{a^2 + L^2} \leq r$ , and in Region III the respective parameter is  $\sqrt{r^2 + L^2}$  because the minimal value of  $r$  there, is  $a$ .

According with the above, the expression for the potential in terms of leading quantities is

$$\begin{aligned} \mathbf{A}_{\text{dip}}^{(o)}(\mathbf{r}) &= \frac{\mu_o}{4\pi} \mathbf{m} \times \hat{\rho} \\ &\times \begin{cases} \frac{\rho}{(r^2 + a^2)^{3/2}}, & 0 < \rho < a; \quad L < |z| \\ \frac{\rho}{(r^2 + a^2)^{3/2}}, & a < \rho; \quad L < |z| \\ \frac{\rho}{(a^2 + L^2)^{3/2}}, & 0 < \rho < a; \quad 0 < |z| < L \\ \frac{\rho}{(r^2 + L^2)^{3/2}}, & a < \rho; \quad 0 < |z| < L. \end{cases} \end{aligned} \quad (12)$$

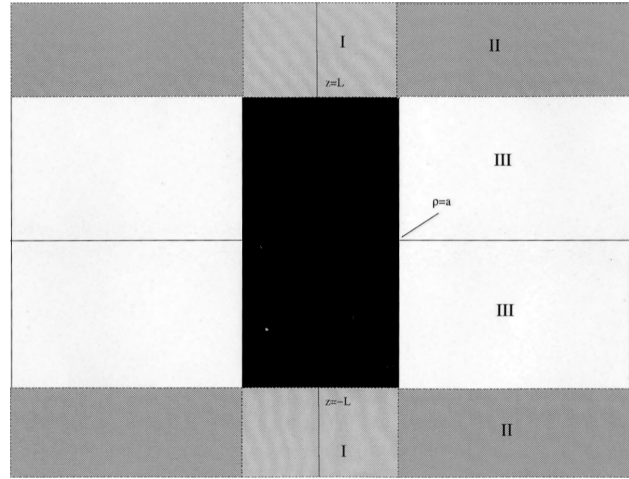


FIGURE 5. The four spatial regions of interest in the case of the cylindrical bobbin of radius  $a$  and height  $2L$ . It is implicitly assumed that for each case the azimuthal angle runs over all of its range  $0 \leq \varphi \leq 2\pi$ .

[The first order corrections to  $A_{\text{dip}}(\mathbf{r})$  are

$$\begin{aligned} 1 - \frac{1}{2} \frac{L^2}{r^2 + a^2}, & \quad 1 - \frac{1}{2} \frac{L^2 + 5a^2}{r^2}, \\ 1 - \frac{1}{2} \frac{15r^2 - 4L^2}{a^2 + L^2}, & \quad \text{and} \quad 1 - \frac{1}{2} \frac{15a^2 - 4L^2}{r^2 + L^2} \end{aligned}$$

for regions I, II, inside cylinder and III, respectively].

From the above expression it can be observed that  $\mathbf{A}_{\text{dip}}(\mathbf{r})$  has a dipolar-like structure which becomes more evident for points very far away from the current. We may also note from (12) that in the limit case of a very long cylinder  $a \ll L$ , this potential has the same structure to the one of the sphere given by Eqs. (6) and (7).

In order to be able of distinguishing whether if  $\mathbf{A}_{\text{dip}}(\mathbf{r})$  as predicted by bobbins method is equal to the Biot-Savart potential

$$\mathbf{A}(\mathbf{r}) = \frac{\mu_o}{4\pi} \int \frac{\mathbf{J}(\mathbf{l})}{|\mathbf{r} - \mathbf{l}|}$$

generated by the cylindrical surface distribution at rotation it is necessary to use numerical methods. This last obeys to the fact that at the moment there is not reported any analytical calculation of these integrals. In Fig. 6 it is plotted the result of performing the numerical integration of  $A(\mathbf{r})$  and then divided by  $A_{\text{dip}}(\mathbf{r})$  against

$$\frac{r}{L} = \sqrt{\epsilon^2 \left(\frac{\rho}{a}\right)^2 + \left(\frac{z}{L}\right)^2}$$

for several values of  $\epsilon = a/L \ll 1$ . The coordinates  $z/L$  and  $\rho/a$  have been chosen to run in the range  $[0, 5]$  in steps of 0.1. From this figure it is evident the good agreement between  $\mathbf{A}_{\text{dip}}(\mathbf{r})$  and  $\mathbf{A}(\mathbf{r})$  except at the edges  $z = -L$  and

$z = +L$  of the cylinder and also on the side  $\rho = a$  of it. These singular discrepancies come mainly from the Biot-Savart expression for the potential where at the side of the cylinder it vanishes  $A(\rho = a, \varphi, z) = 0$  while for  $|z| = L$  the divergence is quite strong since it goes as  $\epsilon \log \epsilon$  being  $\epsilon \ll 1$ . For this reason these values were not included in Eq. (12). The physical explanation about the null value of  $\mathbf{A}(\mathbf{r})$  at the boundary  $\rho = a$  comes from the fact that always on the surface of a perfect conductor the magnetic field  $\mathbf{B}$  is zero providing that only tangential  $\mathbf{B}$  fields can exist [4] which is precisely the case. On the other hand, the steep value for  $\mathbf{A}(\mathbf{r})$  at  $|z| = L$  arise as a consequence that we have assumed a cylindrical shell of finite height  $2L$  consequently it does not have physical lids but it has hollows which deform strongly both the line fields and the intensity of the  $\mathbf{B}$  field. Once it is clarified the above we can conclude reasonably from Figure 6 that the potential generated by a uniform distribution of electric charge on a cylindrical shell at rotation is equal to a dipolar vector potential produced by a cylindrical bobbin of  $N$  turns.

### 3.3. Rotating ellipsoid

As a last example of the efficiency of the bobbins method let us find the vector potential generated by a charge  $Q$  uniformly distributed on the surface of an ellipsoid (of revolution) of height  $2c$  and major axis  $2a$  which is spinning round at uniform angular velocity  $\omega$  along its symmetry ( $Z$ -)axis. The calculation for  $\mathbf{A}(\mathbf{r})$  in this case is not so difficult as apparently it seems to be if one notes that under a transformation of coordinates from the usual set  $\{x, y, z\}$  to the hat set  $\{\hat{X}=x/a, \hat{Y}=y/a, \hat{Z}=z/c\}$ , the equation of the ellipsoid  $\rho^2/a^2 + z^2/c^2 = 1$  becomes the equation of a sphere of radius  $\hat{R} = 1$ , that is  $\hat{\rho}^2 + \hat{Z}^2 = 1$ , where  $\rho = \sqrt{x^2 + y^2}$  and  $\hat{\rho} = \sqrt{\hat{X}^2 + \hat{Y}^2}$  respectively. Under this transformation the ellipsoidal problem is now reduced to the well known case of the spherical geometry (in hat coordinates in this case) which is given by Eqs. (6) and (7) and whose hat version is

$$\mathbf{A}(\mathbf{r}) = \frac{\mu_0 \hat{R} \hat{\sigma} \hat{\omega}}{3} \hat{\varphi} \begin{cases} \hat{\rho} & 0 < \hat{r} \leq \hat{R}, \\ \frac{\hat{R}^3}{\hat{r}^3} \hat{\rho} & \hat{R} < \hat{r}. \end{cases} \quad (13)$$

It is worth it to remark at this point that the above expression is the one we are looking for providing the electrical charge  $Q$  is the same on both surfaces.

To give an explicit expression for (13) in terms of the usual set of coordinates it is necessary first to state the relations between the hat and non-hat physical quantities involved in the problem. To begin with the azimuthal angle does not change the

$$\varphi = \arctan \frac{y}{x} = \arctan \frac{\hat{Y}}{\hat{X}} = \hat{\varphi}$$

consequently the respective angular velocity  $\omega = d\varphi/dt$  will not change also. The first consequence of this is that current

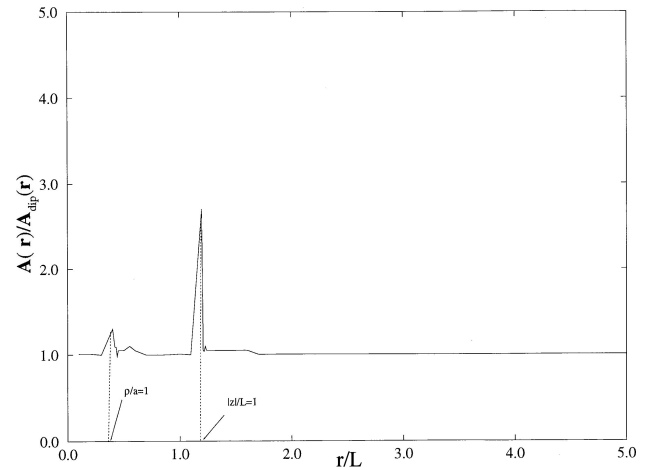


FIGURE 6. Numerical value of the Biot-Savart potential  $\mathbf{A}(\mathbf{r})$  for the case of cylindrical geometry divided by the dipolar potential  $\mathbf{A}_{dip}(\mathbf{r})$  of the respective bobbin all as a function of  $r/L$  and for several values of  $\epsilon = a/L \ll 1$ .

must be the same in both sets of coordinates  $I = \hat{I} = Q\omega/(2\pi)$ . The surface of the unitary sphere is  $\hat{S} = 4\pi$  and from  $Q = \hat{Q} = \hat{\sigma} \hat{S} = \sigma S$  it follows that  $\hat{\sigma} = \sigma(S/\hat{S})$  where

$$S(e) = \frac{2\pi a^2}{\sqrt{1-e^2}} \ln \left( \frac{1 + \sqrt{1-e^2}}{1 - \sqrt{1-e^2}} \right)$$

is the ellipsoid area and  $e = a/c$  its eccentricity. If the density current generated by the rotating ellipsoid is

$$\mathbf{J}(\mathbf{l}) = \delta(r' - r_o) \sigma \omega \rho' \hat{\varphi}'$$

where  $\rho' = r' \sin \theta'$  and

$$r_o = \frac{a}{\sqrt{1 - (1 - e^2) \cos^2 \theta'}}$$

then its magnetic moment will be

$$\begin{aligned} \mathbf{m} &= \frac{1}{2} \int d^3\mathbf{l} \mathbf{l} \times \mathbf{J}(\mathbf{l}) \\ &= \pi a^4 \sigma \omega F(e) \hat{\mathbf{k}}, \end{aligned} \quad (14)$$

where

$$F(e) = \frac{2\sqrt{1-e^2} - e^2 \ln \left( \frac{1 + \sqrt{1-e^2}}{1 - \sqrt{1-e^2}} \right)}{(1 - e^2)^{3/2}}. \quad (15)$$

The corresponding magnetization associated to the rotating ellipsoid is

$$\mathbf{M}_{elips} = \frac{\mathbf{m}}{\frac{4}{3}\pi a^2 c} = \frac{3}{4} e a \sigma \omega F(e) \hat{\mathbf{k}}. \quad (16)$$

[In the limit case of an sphere where  $a=c=R$  and  $e=a/c=1$ , the area becomes

$$S = \lim_{e \rightarrow 1} a^2 \int_{\varphi=0}^{\varphi=2\pi} d\varphi \int_{x=-1}^{x=1} \frac{dx}{1 - (1 - e^2)x^2} = 4\pi R^2$$

while for  $e = 0$  which corresponds to the degeneration of the ellipsoid into an infinite line (namely either of the straight lines  $c \rightarrow \infty$  or  $a \rightarrow 0$ ), the area diverges].

Let us observe that in the limit case of a sphere  $a=c=R$  (i.e.  $e=1$ ) the current is  $\mathbf{J}(\mathbf{l}) = \delta(r' - R)\sigma\omega R \sin\theta' \hat{\varphi}'$  and  $F(e = 1) = 4/3$  with which (16) reduces consistently to (3). Using the relations between the hat and non hat quantities in (13) the potential can be written as

$$\mathbf{A}_{\text{dip}}(\mathbf{r}) = \frac{\mu_o}{16\pi^2 a^4} \frac{S(e)}{F(e)} \mathbf{m} \times \hat{\rho} \times \begin{cases} \rho/a & 0 < \sqrt{(\frac{\rho}{a})^2 + (\frac{z}{c})^2} \leq 1, \\ \frac{1}{[(\frac{\rho}{a})^2 + (\frac{z}{c})^2]^{3/2}} \frac{\rho}{a} & 1 < \sqrt{(\frac{\rho}{a})^2 + (\frac{z}{c})^2}. \end{cases} \quad (17)$$

where  $S(e)$  is the ellipsoid area and  $F(e)$  is given by (15).

For the rotating ellipsoid, the analytical solution of the corresponding Biot-Savart equation

$$\mathbf{A}(\mathbf{r}) = \frac{\mu_o}{4\pi} \int \frac{\mathbf{J}(\mathbf{l})}{|\mathbf{r} - \mathbf{l}|}$$

has not been done so far, consequently it is also necessary in this case to use numerical methods in order to check the coincidence between the values of Eq. (17) and  $\mathbf{A}(\mathbf{r})$ . In Fig. 7 we have plotted the result of integrating numerically Biot-Savart equation for several values of the eccentricity  $e$  of the ellipsoid. As it is seen from such a figure there is a very good agreement between  $\mathbf{A}(\mathbf{r})$  and  $\mathbf{A}_{\text{dip}}(\mathbf{r})$  whence it is possible to conclude that the bobbin method also works in this case. We may observe that similarly as it happened in the above case of the cylinder, the coil method allows us also to calculate the vector potential associated to the ellipsoidal superficial distribution of electric charge at uniform rotation in both a simpler and precise way.

### 4. Conclusions

By observing that the potential of the sphere given by Eqs. (6) and (7) can be written in terms of the magnetic moment as

$$\mathbf{A}(\mathbf{r}) = \frac{\mu_o}{4\pi} \frac{\mathbf{m} \times \hat{\rho}}{R^3} \begin{cases} \rho & 0 < r \leq R \\ \frac{R^3}{r^3} \rho & R < r, \end{cases} \quad (18)$$

from this equation altogether with Eqs. (11), and (17) it results evident that the magnetic potentials generated by the three superficial distributions at rotation considered in this work have in common a dipolar-like structure.

Concerning in particular to the cylindrical distribution let us observe that in the limit case of a very long cylinder  $a \ll L$  there would be just two regions of interest, namely the inner and the external (Region III) parts to the cylinder,

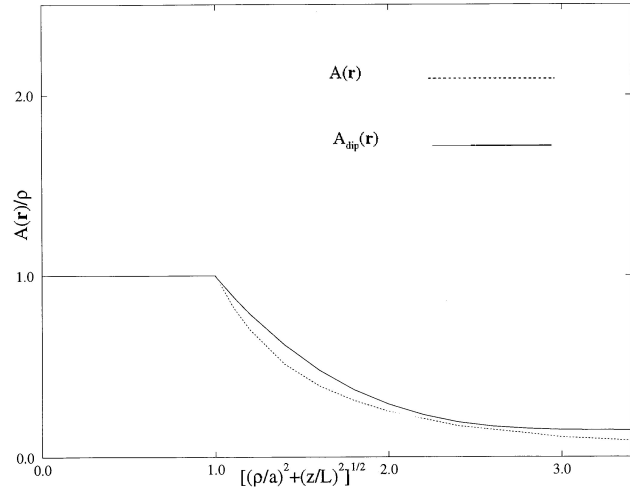


FIGURE 7. Numerical value of  $\mathbf{A}(\mathbf{r})a/\rho$  in the case of the ellipsoidal shell ( continued line ) and the respective dipolar potential  $\mathbf{A}_{\text{dip}}(\mathbf{r})$  (dotted line) both as a function of  $\sqrt{(\rho/a)^2 + (z/L)^2}$  for several values of the eccentricity ( $0 < e = a/c < 1$ ).

and in this limit case the potential (12) becomes

$$\mathbf{A}_{\text{dip}}^{(o)}(\mathbf{r}) \simeq \frac{\mu_o}{4\pi} \frac{\mathbf{m} \times \hat{\rho}}{L^2} \epsilon \begin{cases} \rho/a & 0 < \rho < a \\ \frac{\rho}{a [1 + (\rho/L)^2]^{3/2}} & a < \rho \end{cases} \quad (19)$$

As it was expected of the symmetry of the problem, in this limit there is not dependence on  $z$ .

It is convenient to stress also that for the cylinder case we have plotted in Fig. 6  $\mathbf{A}(\mathbf{r})/\mathbf{A}_{\text{dip}}(\mathbf{r})$  and not  $\mathbf{A}(\mathbf{r})$  against  $r/L$ , this obeys to that in (12) there are involved many regions in the partition of the space and it is easier to see the behavior of the potential in this way. However, for the limit case of a very long cylinder  $a \ll L$  it is worth it to verify numerically whether if the dipolar potential  $\mathbf{A}_{\text{dip}}(\mathbf{r})$  as it is given by (12) is the same to the respective Biot-Savart potential  $\mathbf{A}(\mathbf{r})$ . The results of these numerical calculations are shown in Fig. 8 where we have plotted  $\mathbf{A}(\mathbf{r})$  and  $\mathbf{A}_{\text{dip}}(\mathbf{r})$  against  $\rho$ . As it is easily seen from this figure these potentials are the same.

Referring to the ellipsoidal distribution at rotation let us observe from Eq. (17) that the respective potential has several particular characteristics, first of all and as it was naturally expected the general expression for  $\mathbf{A}(\mathbf{r})$  must have an strong dependence on the eccentricity  $e$ . In addition to this  $\mathbf{A}(\mathbf{r})$  depends on both coordinates  $\rho/a$  and  $z/c$  and not on  $\rho$  and  $z$ . In the limit case where the ellipsoid becomes a sphere ( $a = c = R$ ), the area of the ellipsoid is  $S = 4\pi R^2$  and Eq. (17) leads consistently to Eq. (18). For a degenerate ellipsoid into an infinity line ( $e = a/c \rightarrow 0$ ) the potential of Eq. (17) diverges.

Concerning to the common characteristics of the potentials (12), (17), and (18) we point out that there basically three which are not difficult of seeing. The first one is that they have azimuthal symmetry which was expected from the symmetric shape of them around  $z$  axis. Another common

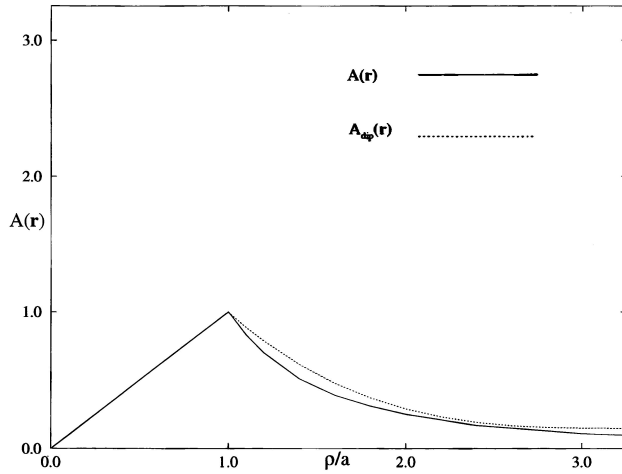


FIGURE 8. Numerical value of  $\mathbf{A}(\mathbf{r})$  for the case of a very long cylinder ( $L \gg a$ ) together with the respective dipolar potential  $\mathbf{A}_{dip}(\mathbf{r})$  both as a function of  $\rho$ .

behaviour is that these potentials vanish along  $z$ -axis ( $\rho = 0$ ), this due to that the current  $\mathbf{J}$  circulates along  $\hat{\varphi}$  direction. Finally let us observe that they behave is such a way that their maximal value, for fixed values of the radial coordinate  $r = ct$ , is reached at the  $XY$ -plane (*i.e.*  $\theta = \pi/2$ ).

Let us calculate now the  $\mathbf{B}$  fields generated by the three rotating surfaces. The expression for the magnetic field generated by the rotating sphere is easily calculated from Eq. (18) and its value is

$$\mathbf{B}_{sph}(\mathbf{r}) = \nabla \times \mathbf{A}(\mathbf{r}) = \frac{\mu_o}{4\pi} \frac{1}{R^3} \begin{cases} 2\mathbf{m}, & 0 < r < R, \\ [3(\mathbf{m} \cdot \hat{\mathbf{r}})\hat{\mathbf{r}} - \mathbf{m}] \frac{R^3}{r^3}, & R < r. \end{cases} \quad (20)$$

The main characteristic of this potential is that it is constant inside the sphere while outside it is dipolar-like, reaching its minimum value for  $r = ct$  at the  $XY$ -plane, while along positive  $Z$  axis has its maximal value.

From Eq. (12) it is found that the  $\mathbf{B}$  field generated by the rotating cylindrical shell is

$$\mathbf{B}_{cyl}(\mathbf{r}) = \nabla \times \mathbf{A}(\mathbf{r}) = \frac{\mu_o}{4\pi} \left[ \frac{3(r^2 + a^2) + L^2}{(r^2 + a^2)^2[r^2 + a^2 + L^2]^{3/2}} (\mathbf{m} \cdot \mathbf{r}) \mathbf{r} + \frac{(z^2 - \rho^2) + 2(r^2 + a^2)(r^2 + a^2 + L^2)}{(r^2 + a^2)^2[r^2 + a^2 + L^2]^{3/2}} \mathbf{m} \right] \\ \simeq \frac{\mu_o}{4\pi} \frac{1}{(a^2 + L^2)^{3/2}} \begin{cases} [3(\mathbf{m} \cdot \hat{\mathbf{r}})\hat{\mathbf{r}} - \mathbf{m}] \frac{(a^2 + L^2)^{3/2}}{(r^2 + a^2)^{3/2}} & 0 < \rho < a; \quad L < |z| \\ [3(\mathbf{m} \cdot \hat{\mathbf{r}})\hat{\mathbf{r}} - \mathbf{m}] \frac{(a^2 + L^2)^{3/2}}{(r^2 + a^2)^{3/2}} & a < \rho; \quad L < |z| \\ 2\mathbf{m} & 0 < \rho < a; \quad 0 < |z| < L \\ [3(\mathbf{m} \cdot \hat{\mathbf{r}})\hat{\mathbf{r}} - \mathbf{m}] \frac{(a^2 + L^2)^{3/2}}{(r^2 + L^2)^{3/2}} & a < \rho; \quad 0 < |z| < L. \end{cases} \quad (21)$$

The structure of this field is quite the same to the one of the sphere, it is constant inside the shell while outside it has a dipolar-like behaviour.

Finally from Eq. (17) the magnetic field for the ellipsoid is

$$\mathbf{B}_{elip}(\mathbf{r}) = \nabla \times \mathbf{A}(\mathbf{r}) = \frac{\mu_o}{16\pi^2 a^5} \frac{S(e)}{F(e)} \\ \times \begin{cases} 2\mathbf{m} & 0 < \sqrt{\left(\frac{\rho}{a}\right)^2 + \left(\frac{z}{c}\right)^2} \leq 1 \\ \frac{[3(\mathbf{m} \cdot \hat{\mathbf{r}})\hat{\mathbf{r}} - \mathbf{m}]}{\left[\left(\frac{\rho}{a}\right)^2 + \left(\frac{z}{c}\right)^2\right]^{3/2}} & 1 < \sqrt{\left(\frac{\rho}{a}\right)^2 + \left(\frac{z}{c}\right)^2}. \end{cases} \quad (22)$$

As it is observed from the above equation,  $\mathbf{B}_{elip}(\mathbf{r})$  has also exactly the same structure than those of the sphere and the ellipsoid.

Once calculated the  $\mathbf{B}$  fields we were looking for, we want to point out that there exist an interesting physical situation where it can be applied present results. Incidentally

we find that the magnetic fields (20), (21), and (22) have interesting features which would be applied to the study of some aspects of the Strong Interactions of Elementary Particles. In Quantum Chromodynamics (QCD) the more accepted theory, of the Strong Interactions of Elementary Particles [5] it is believed that intense Chromo Magnetic Fields are generated inside hadrons which confine quarks inside them. Nowadays, it is well known that one of the central problems of QCD is about the precise structure of the confining potentials. Although many phenomenological potentials have been proposed in the literature accounting for such a property, however the most extensively used in meson phenomenology is the following

$$V(r) \equiv V_{Coul}(r) + V_{conf}(r) = -\frac{\xi}{r} + \kappa r, \quad (23)$$

The first term  $V_{Coul}$  in (23) is a color Coulomb potential which accounts for the spectra while the other  $V_{conf}$  a linear one, accounts for quark confinement [This is due that it accounts successfully for quark confinement besides of reproducing very well almost all of the mesonic spectra [6–8]].

According with the present approach whose main features are given by Eqs. (20) (21), and (22) it is possible to

show that (23) must be necessarily the structure of a quark-quark potential inside a meson if we think of it as an spherical colorless particle containing a quark ( $q$ ) and anti-quark ( $\bar{q}$ ) on whose surface is uniformly distributed a color charge  $Q$  (assigned to the quark  $q$ ) which is rotating at a constant velocity and where a point-like color charge  $-Q$  (corresponding to an anti-quark  $\bar{q}$ ) is at rest on the center of the sphere (origin of coordinates).

Concerning to the confining part of (23), it arises due that as it is seen from Eq. (20) the chromo  $\mathbf{B}_c$  field inside hadron must be constant, proportional to its magnetic moment, and directed along  $z$ -axis. Effectively, since the respective non Abelian chromo electric field  $\mathbf{E}_c$  must be also constant inside hadrons and it must be on the  $XY$ -plane, that is

$$\mathbf{E}_c = -\omega\mathbf{B}_c \times \hat{\varphi} = -\omega B_c \hat{\varphi}$$

where  $\omega B_c = ct$  is its intensity, this makes that the structure of the scalar chromo potential inside hadrons induced by the rotating color charge  $Q$  must be linear, that is

$$V_{\text{conf}}(\mathbf{r}) = \kappa r. \quad (24)$$

On the other hand the Coulomb-like part of (23) comes from the point-like color charge placed at the origin and it must be of the form

$$V_{\text{Coul}}(\mathbf{r}) = -\frac{\xi}{r}. \quad (25)$$

The two above equations together with Superposition Principle guarantee the consistence of the mesonic potential given by Eq. (23).

Referring to the assumed spherical shape for a meson, it is worthwhile to observe that Eqs. (24) and (25) would have been derived anyway if instead we were assumed that the meson was either cylindrical or elipsoidal. A good example of the independence of these last equations on the shape of the meson (either spherical, cylindrical or elipsoidal) is that found in Ref. 9 where it was shown successfully that if one thinks of a meson as a relativistic cylindrical tube flux it leads to a reliable values of the so called Isgur-Wise function describing hydrogen-like mesonic systems where one of the quarks is very heavy and the other is very light.

From the discussed above we want to conclude the present work by saying that the bobbins method allows to calculate in a simple way the previously unsolved magnetic fields generated by the spherical, elipsoidal, and cylindrical charged surfaces at constant rotation. These  $\mathbf{B}$  fields are the dipolar fields generated by the bobbins and they are constant inside the shells while outside they have a dipolar-like structure. We have also found that Eqs. (24) and (25) are a good example of a possible theoretical utility of the present study.

## Acknowledgment

We want to thank to N. A. and J. E. without whose unvaluable comments would not be possible this work. We acknowledge to PROMEP-SEP and SNI.

- 
1. D.J. Griffiths, *Introduction to Electrodynamics* 2nd Edition, (Prentice Hall, New Jersey 1989).
  2. A.D. Alexeiev, *Problemas de Electrodinámica Clásica*, (MIR, Moscú 1977).
  3. P. Lorrain, D.R. Corson and F. Lorrain *Electromagnetic Fields and Waves* 2nd Edition, (W.H. Freeman 1988).
  4. J.D. Jackson, *Classical Electrodynamics*, 2nd Edition, (J. Wiley & Sons, New-York, Chichester, Brisbane, Toronto 1975).
  5. I.A. Aitchison and J.G. Hey, *Gauge Theories in Particle Physics (A Practical Introduction)*, 2nd Edition, (A. Hilger, Bristol and Philadelphia 1989).
  6. K. Johnson, *Act. Phys. Polon.* **B6** (1975) 865.
  7. W.A. Ponce, *Phys. Rev.* **D19** (1979) 197.
  8. M.G. Olsson, S. Veseli, and K. Williams, *Phys. Rev.* **D51** (1995) 5079.
  9. M.G. Olsson and S. Veseli, *Phys. Rev.* **D51** (1995) 2224.